

Effect of skin-penetrating enhancers on the thermophysical properties of cholesteryl oleyl carbonate embedded in a thermo-responsive membrane

SHAN-YANG LIN*, MEI-JANE LI, HSIU-LI LIN

Biopharmaceutics Laboratory, Department of Medical Research and Education, Veterans General Hospital-Taipei, Taipei, Taiwan
E-mail: sylin@vghtpe.gov.tw

The effect of skin-penetrating enhancers such as propylene glycol (PG), Azone and ethanol on the thermophysical properties of cholesteryl oleyl carbonate (COC) was investigated using differential scanning calorimetry (DSC) and microscopic Fourier-transform infrared (FT-IR) spectroscopy. The results indicate that PG did not influence the DSC thermograms and IR spectra of COC in the different ratios of COC and PG mixture; whereas Azone interacted with COC not only to lower the semectic-cholesteric phase transition temperature of COC but also to induce a new IR spectral peak at 1653 cm^{-1} which shifted from the carbonyl stretching band (1636 cm^{-1}) of Azone. Ethanol did not interact with COC, but it influenced the IR spectral peak intensity of COC at 1253 cm^{-1} . The peak intensity at 1253 cm^{-1} gradually rose with the time of ethanol evaporation and was similar to that of the temperature effect. The solubility parameter was also used to explain the miscibility and interaction between COC and PG, Azone or ethanol.

© 2000 Kluwer Academic Publishers

1. Introduction

Recently, we have successfully developed a novel highly thermo-sensitive membrane-embedding liquid crystal to switch drug delivery in a pulsatile fashion [1–10]. Cholesteryl oleyl carbonate (COC), a kind of cholesteric liquid crystal (Fig. 1), was embedded into an artificial membrane to give a thermo-responsive function. We also found that the on-off switching penetration behavior of this thermo-responsive membrane was not influenced by changing the pH of the medium or the type of medium [10].

It is well known that skin-penetrating enhancers have been used for several years to improve the percutaneous absorption of drugs. Their significance has become greater with the development of transdermal delivery [11]. The mechanism of skin-penetrating enhancers is very complicated, but the perturbation of the lipid structure in stratum corneum caused by these enhancers has been recognized to be the predominant factor [11–13]. COC has an oleyl group like the carboxylic acids with long-chain hydrocarbon side groups in the lipid structure of stratum corneum. Thus whether the skin-penetrating enhancer causes disorder or interacts with the molecular structure of COC is unclear. When the COC-embedded membrane is applied as a control membrane of the transdermal drug delivery system, the skin-

penetrating enhancers contained in topical formulations may alter the structure of COC to destroy the on-off switching function of the COC-embedded membrane and is worthy of investigation. Thus, the aim of this preliminary study is to investigate the effect of skin-penetrating enhancers on the thermophysical properties of COC.

2. Materials and methods

2.1. Materials

COC was purchased from Sigma Chemical Co. (St. Louis, MO, USA) and used without further purification. Skin-penetrating enhancers such as ethanol, propylene glycol (PG) (Nacalai Tesque Inc., Kyoto, Japan) and Azone (Whitby Res. Inc., Virginia, USA) were used. All other reagents and chemicals were reagent grade products.

2.2. Sample preparations for infra-red and thermal determinations

(1) Different ratios (wt/wt,%) of COC and each skin-penetrating enhancer were mixed in a test tube and vortexed for 2 h at $25\text{ }^{\circ}\text{C}$. Each mixture and raw material

*Author to whom all correspondence should be addressed.

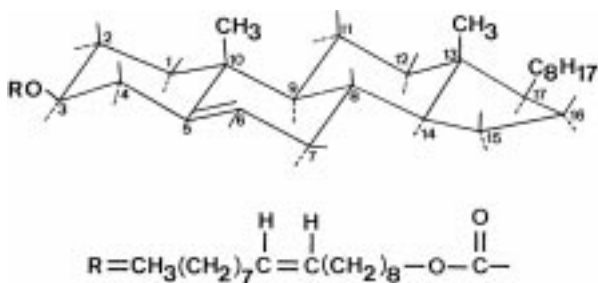


Figure 1 Chemical structure of cholesteryl oleyl carbonate (COC).

were used for infra-red (except the ethanol group) and thermal determinations.

(2) COC was previously dissolved in chloroform and then cast on a CaF_2 disk. After evaporation of the chloroform, COC film cast on CaF_2 was immersed in ethanol for 2 h and then withdrawn (as an ethanol group). Residual ethanol gradually evaporated under a blowing condition; the infra-red spectra of COC films were determined at each prescribed interval. After one hour of evaporation, hot air (50°C) was purged.

2.3. Thermal analysis

A differential scanning calorimeter (DSC-910, TA Instruments, USA) was used to determine the thermal properties of all the samples. The heating rate was $2^\circ\text{C}/\text{min}$ from 5 to 50°C , with an open pan system under a stream of N_2 gas flow. The instrument was calibrated with indium [1–3].

2.4. Micro Fourier-transform infra-red (FT-IR) spectroscopic studies

Infra-red spectra of all the samples were detected using an FT-IR microscopic spectrometer (Micro FTIR-200, Jasco Co., Tokyo, Japan) equipped with an MCT detector using a transmission technique [1–3]. The IR spectra were taken at 4 cm^{-1} spectral resolution and generally 200 scans were accumulated to get a reasonable signal-to-noise ratio. The aperture size employed was about $10\ \mu\text{m} \times 10\ \mu\text{m}$.

3. Results and discussion

In order to understand whether the skin-penetrating enhancer can influence the thermophysical behavior of COC to destroy the on-off function of COC embedded in a membrane, the effect of the skin-penetrating enhancer on the COC has been studied by thermal and FT-IR spectroscopic analyzes. The IR spectra of COC at 25 and 4°C are shown in Fig. 2. The peaks at 2928 and 2855 cm^{-1} assign to asymmetric and symmetric CH_2 stretching vibrational modes, and two shoulders at 2951 and 2869 cm^{-1} are due to asymmetric and symmetric CH_3 stretching vibrational modes, respectively. The peak at 1740 cm^{-1} corresponds to a $\text{C}=\text{O}$ carbonyl stretching band, and the peak at 1466 cm^{-1} assigns to CH_2 scissoring and stretching bands [14]. The peak near $1265 - 1253\text{ cm}^{-1}$ is due to methylene wagging and twisting vibrations but also assigns to the $\text{C}-\text{O}$

stretching mode of the carbonate ester in COC. It is evident that the peak intensity at $1265 - 1253\text{ cm}^{-1}$ for COC at 25°C is markedly higher than that at 1466 cm^{-1} (Fig. 2a), even though wagging and twisting vibration bands are generally weaker than those resulting from methylene scissoring. The $\text{C}-\text{O}$ stretching mode of the carbonate ester of COC might be responsible for this intense absorption. However, the $\text{C}-\text{O}$ stretching mode of carbonate ester in COC contributes less at 4°C , as shown in Fig. 2b. This might be because the COC at 4°C was below the smectic-cholesteric phase transition temperature (15.3°C) of COC. A significantly increased intensity for $1265 - 1253\text{ cm}^{-1}$ at a higher temperature indicates the dominant contribution of the $\text{C}-\text{O}$ stretching mode of the carbonate ester in COC (Fig. 2a). The $\text{C}-\text{O}$ stretching mode of the carbonate ester in COC increased its intensity at a higher temperature due to a significantly altered dipole moment of the $\text{C}-\text{O}-\text{C}$ band vibration [15]. In our previous study [1], we also found that the peak intensity at $1265 - 1253\text{ cm}^{-1}$ for COC suddenly increased from the smectic-cholesteric phase transition temperature of COC. Fig. 3a shows the DSC thermogram of COC. Obviously, two endothermic peaks at 15.33°C and 34.70°C were observed, which is somewhat different from our previous results at 18.3°C and 37.5°C [1–3]. Different heating rates of DSC determination might cause these temperature variations [1, 16]. The former may be due to the smectic-cholesteric phase transition temperature with an enthalpy of 1.03 J/g , the latter corresponds to the melting point of COC and is also the cholesteric-isotropic phase transition temperature with an enthalpy of 0.86 J/g [1, 17].

The effect of PG on the DSC curves and IR spectra of COC in the mixture of COC and PG is shown in Figs 3 and 4. It clearly indicates that PG has an endothermic peak at 157.48°C (Fig. 3f), which corresponded to the melting point of PG. Two endothermic peaks near 15°C and 34°C were also observed from the DSC curves of the different ratios of

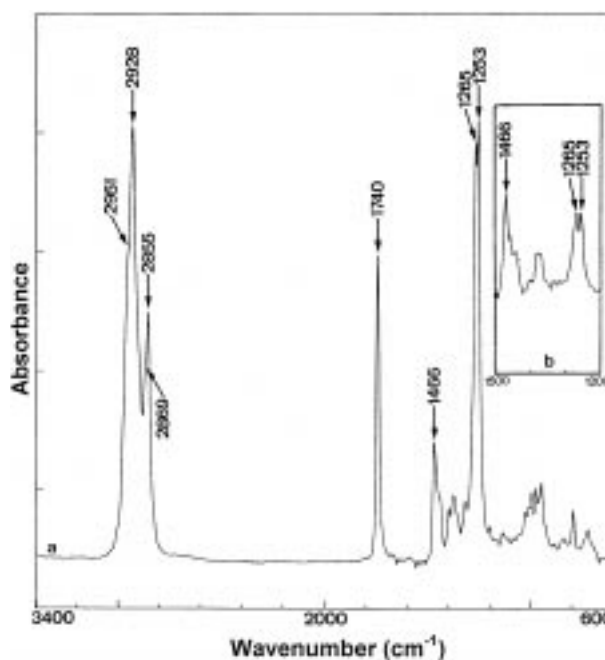


Figure 2 FT-IR spectra of COC at 25°C (a) and 4°C (b).

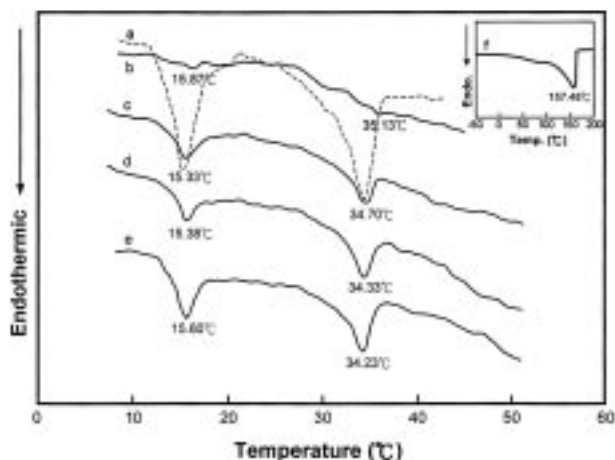


Figure 3 Effect of PG on the DSC curves of COC in their mixtures. Key: Mixing ratio of COC and PG: (a) COC 100%; (b) 50% : 50%; (c) 66.67% : 33.33%; (d) 80% : 20%; (e) 90% : 10%; (f) PG 100%.

COC and PG although the 1:1 mixture exhibited a less intense DSC curve, which was approximately near the endothermic peaks of the intact COC. Moreover, the enthalpy value for the endothermic peak at 15 or 34 °C was also almost equal to that of the 1.03 or 0.86 J/g of the COC. This suggests that PG did not influence the thermophysical property of COC. The IR spectra also confirmed this result (Fig. 4A). The solubility parameter can also be used to explain this result. It has frequently been found that polymers dissolve in solvents having solubility parameters within about one unit of their own [18]. In this study, the solubility parameters of PG and COC are about 12.6 and 9.14 (calculated), respectively [19]. This reveals that COC was immiscible with PG, suggesting there was a lack of interaction between COC and PG.

Azone (1-dodecylazacycloheptan-2-one) has been shown to be a very effective enhancer of skin

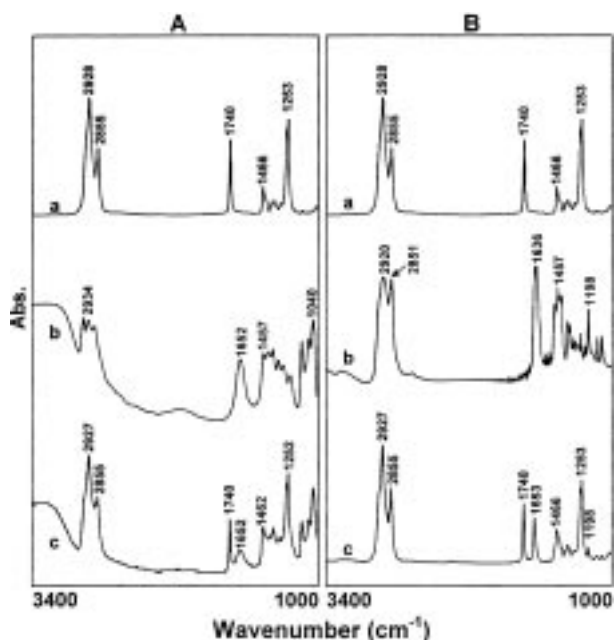


Figure 4 Effect of PG (A) or Azone (B) on the FT-IR spectra of COC in their mixtures. Key: (a) COC; (b) PG or Azone; (c) 80% COC : 20% PG (Azone).

permeability [11–13]. The mechanism of action for Azone to enhance skin permeability is still unknown, but disrupting the lipid structure of the horny layer may be supposed [12, 13, 20]. When the COC-embedded membrane is applied as a control membrane for the transdermal drug delivery system with Azone as an enhancer, whether Azone can affect the on-off function of COC in membrane is suspicious. The effect of Azone on the COC was studied and evidenced from the changes in DSC thermograms and IR spectra. Azone shows an endothermic peak at 4.83 °C. Once the COC was mixed with Azone at different ratios, two endothermic peaks of COC at 15 °C and 34 °C significantly shifted to a lower range of temperatures when the amount of Azone used was increased (Fig. 5). Furthermore, a new peak at 1653 cm^{-1} was found in the IR spectra of the mixture of COC and Azone (Fig. 4B). This new peak at 1653 cm^{-1} might be attributed to the peak shift from 1636 cm^{-1} assigned to the carbonyl stretching band of Azone. This shifting phenomenon demonstrates that an interaction between COC and Azone occurred. It is also possible to explain the interaction using the solubility parameter. The solubility parameter of Azone is about 9.06 [20], which was very close to the 9.14 parameter of COC. Since the numbers are within one unit, COC would be expected to dissolve readily in Azone. COC easily dissolved in Azone to improve their interaction and resulted in the appearance of a new IR spectral peak at 1653 cm^{-1} .

Fig. 6 shows the effect of ethanol on the DSC thermograms of COC in the mixture of COC and ethanol. No endothermic peak appeared on the DSC curve with a higher percentage of ethanol in the mixture. Once the amount of COC increased, the endothermic peak appeared but was at the lower temperature range, depending on the amount of ethanol added. When the amount of COC used was > 80% in the mixture, both endothermic peaks were close to the original endothermic peaks at 15 °C and 34 °C of COC (Fig. 6e). The endothermic peak of the mixture of COC and ethanol which appeared at the lower temperature range might be because the COC was softened by hot

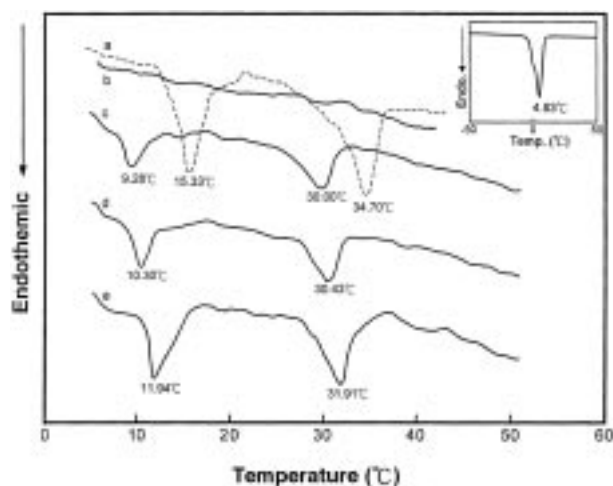


Figure 5 Effect of Azone on the DSC curves of COC in their mixtures. Key: Mixing ratio of COC and Azone: (a) 100% : 0; (b) 80% : 20%; (c) 90.0% : 10%; (d) 95% : 5%; (e) 98% : 2%.

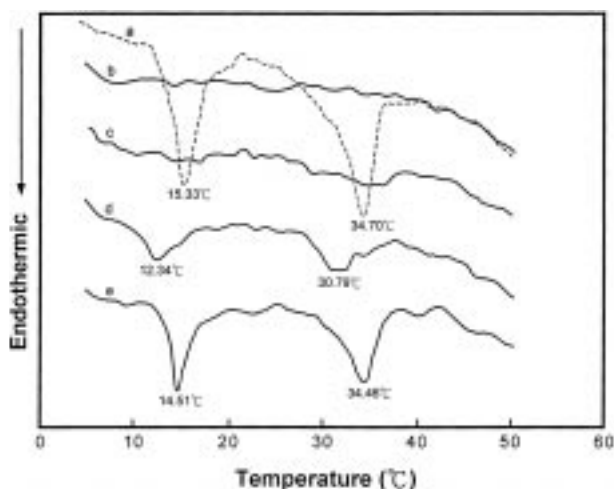


Figure 6 Effect of ethanol on the DSC curves of COC in their mixtures. Key: Mixing ratio of COC and ethanol: (a) 100% : 0; (b) 80% : 20%; (c) 90.0% : 10%; (d) 95% : 5%; (e) 98% : 2%.

ethanol during heating. The fact is that ethanol was immiscible with COC, which was also confirmed by different values of the solubility parameter. The solubility parameter of ethanol is about 12.7 [19], which is clearly different from the value of 9.14 of COC. The immiscible property of ethanol and COC resulted in the lack of interaction between them. Fig. 7A indicates the time-dependent IR spectral changes of COC via gradual evaporation of the residual ethanol from the COC film cast on a CaF_2 disk. It clearly shows that the peak intensity of 1253 cm^{-1} at the initial stage of ethanol was smaller than that of the original peak intensity of 1253 cm^{-1} for the intact COC. By increasing the time of ethanol evaporation, the peak intensity at 1253 cm^{-1} gradually increased. As shown in Fig. 7B, the value of the peak intensity ratio between 1253 cm^{-1} and 1466 cm^{-1} initially decreased and then gradually increased to reach a constant value. When the sample was purged by hot air, the peak intensity ratio was greater.

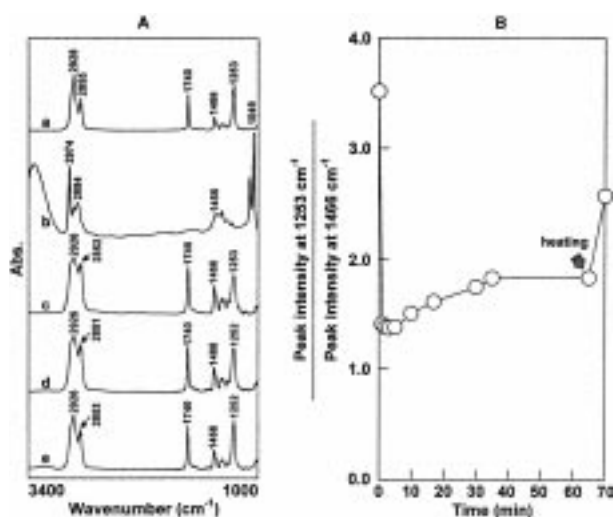


Figure 7 Time-dependent IR spectral change of COC via gradual evaporation of the residual ethanol from the COC film cast on a CaF_2 disk. Key: (A) Time for ethanol evaporation: (a) COC; (b) ethanol; (c) 5 min; (d) 30 min; (e) 70 min. (B) Changes in peak intensity ratio of $1253\text{ cm}^{-1}/1466\text{ cm}^{-1}$.

According to the IR results in Fig. 2 and our previous study [1], the peak intensity at 1253 cm^{-1} of COC was temperature-dependent; below the smectic-cholesteric phase transition temperature it was smaller but above the smectic-cholesteric phase transition temperature it was larger. In the present study, however, the peak intensity of 1253 cm^{-1} gradually rose with the time of ethanol evaporation and was similar to that of the temperature effect. The reason is unclear, but the lowered temperature of COC induced by the evaporation process of ethanol might be responsible for this result. The sudden increase in the peak intensity ratio after introduction of hot air suggests that the C—O stretching mode of the carbonate ester in COC was more sensitive to the temperature effect. From the above result, whether the skin-penetrating enhancer indeed influences the on-off switching function of the COC-embedded membrane needs to be studied in the future.

Acknowledgments

This work was supported by the National Science Council, Taipei, Taiwan (NSC-87-2314-B075-032 and NSC-88-2314-B075-005).

References

1. Y. Y. LIN, K. S. CHEN and S. Y. LIN, *J. Chin. Chem. Soc.-Taipei* **42** (1995) 865.
2. *Idem. Biomed. Engineer. Appl. Bas. & Commun.* **7** (1995) 502.
3. *Idem. Int. J. Pharm.* **124** (1995) 53.
4. S. Y. LIN, Y. Y. LIN and K. S. CHEN, *Drug Delivery* **2** (1995) 123.
5. *Idem. Pharm. Pharmacol. Lett.* **5** (1995) 159.
6. K. S. CHEN, Y. Y. LIN and S. Y. LIN, *Drug Delivery System (Japan)* **11** (1996) 55.
7. Y. Y. LIN, K. S. CHEN and S. Y. LIN, *J. Control. Rel.* **41** (1996) 163.
8. S. Y. LIN, Y. Y. LIN and K. S. CHEN, *Pharm. Res.* **13** (1996) 914.
9. S. Y. LIN, K. S. CHEN, Y. Y. LIN and M. J. LI, *Pharm. Pharmacol. Lett.* **6** (1996) 131.
10. S. Y. LIN, K. S. CHEN and Y. Y. LIN, *J. Control Rel.* **55** (1998) 13.
11. K. A. WALTERS and J. HADGRAFT, "Pharmaceutical Skin Penetration Enhancement" (Marcel Dekker, Inc., New York, 1993).
12. B. W. BARRY, *J. Control. Rel.* **6** (1987) 85.
13. *Idem., ibid.* **15** (1991) 237.
14. M. JACKSON and H. H. MANTSCH, *Spectrochim. Acta Rev.* **15** (1993) 53.
15. D. G. CAMERON, H. I. CASAL and H. H. MANTSCH, *Biochemistry*, **19** (1980) 3365.
16. G. W. GRAY and M. HANNANT, *Mol. Cryst. Liq. Cryst.* **53** (1979) 263.
17. P. H. KEYES and A. J. NICASTRO, *Mol. Cryst. Liq. Cryst.* **67** (1981) 59.
18. L. H. SPERLING, "Introduction to Physical Polymer Science" (John Wiley & Sons, New York, 1992), Ch. 3, pp. 65–121.
19. J. BRANDRUP and E. H. IMMERGUT, "Polymer Handbook" (John Wiley & Sons, New York, 1989), 3rd Edn, Ch. 7, pp. 519–559.
20. K. A. WALTERS and J. HADGRAFT, "Pharmaceutical Skin Penetration Enhancement" (Marcel Dekker, Inc., New York, 1993), Ch. 7, pp. 175–197.

Received 9 June
and accepted 10 December 1999